Supporting information

Understanding the mechanism by which Gd(III) coiled coils achieve magnetic resonance relaxivity - a study into the water coordination chemistry

S. L. Newton,[a,b] A. Franke,[c,d] A. Zahl,[c] G. Molinaro,[a] A. Kenwright,[e] D. J. Smith,[f] I. Ivanovic-Burmazovic,[c,d*] M. M. Britton,[a*] A. F. A. Peacock[a*]

[a] School of Chemistry, University of Birmingham, Edgbaston, B15 2TT, UK

[b] PSIBS, School of Chemistry, University of Birmingham, Edgbaston, B15 2TT, UK

[c] Department Chemie und Pharmazie, Universität Erlangen-Nürnberg, D-91058, Erlangen Germany

[d] Department of Chemistry, Ludwig-Maximilians-Universität München Butenandtstr. 5-13, 81377 München, Germany

[e] School of Chemistry, Durham University, Durham, DH1 3LE, UK

[f] School of Mathematics, University of Birmingham, Edgbaston, B15 2TT, UK

*e-mail: m.m.britton@bham.ac.uk and a.f.a.peacock@bham.ac.uk

Contents:

Materials and Methods and 10 Supplementary Figures

1. Materials and Methods

Fmoc protected amino acids, dimethylformamide and N,N,N',N'-tetramethyl-O-(1H-benzotriazol-1-yl)uronium hexafluorophosphate (HBTU) were purchased from Pepceuticals Ltd. Rink amide MBHA resin, diisopropylethylamine (DIPEA), N-methylpyrrolidone (NMP), triisopropylsilane (TIPS) and trifluoroacetic acid (TFA) were purchased from AGTC Bioproducts Ltd. $GdCl_3 \cdot 6H_2O$ and $TbCl_3 \cdot 6H_2O$ were obtained from Sigma Aldrich. Xylenol orange indicator, urea, guanidinium hydrochloride, glacial acetic acid, ethylenediaminetetraacetic acid (EDTA) and 4-(2-hydroxyethyl)-1-piperazineethanesulfonic acid (HEPES), were purchased from Fisher Scientific Ltd. D_2O was purchased from VWR. ^{17}O enriched water was purchased from D-Chem Ltd. Tel Aviv, Israel.

Peptide Synthesis and Purification

Peptides were synthesised on a CEM Liberty Blue automated peptide synthesiser on rink amide MBHA resin (0.25 mmol scale, 0.65 mmol g^{-1}) using standard Fmoc-amino acid solid-phase synthesis protocols.[1] The peptides were purified and characterised as previously reported.[2]

Sample Preparation

Stock solutions of $GdCl_3$ and $TbCl_3$ (1 mM) were freshly prepared in deionized water and their concentrations determined in triplicate using a xylenol orange and EDTA titration, as previously reported by Fedeli and co-workers.[3] Peptide stock solutions were freshly prepared and concentrations determined in triplicate, based on the tryptophan absorbance at 280 nm (ε_{280} = 5690 $M^{-1}cm^{-1}$) in 6 M aqueous urea.

Circular Dichroism (CD) Spectroscopy

CD spectra for solutions containing 30 μM peptide monomer in the absence and presence of 10 μM $GdCl_3$, in 10 mM HEPES buffer pH 7.0, were recorded in a 1 mm path length quartz cuvette on a Jasco J-715 spectropolarimeter after 20 minutes equilibration. The observed ellipticity in millidegrees was converted into molar ellipticity, (Θ), and is reported in units of deg $dmol^{-1}$ cm^2. The percentage folding was calculated based on the theoretical maximum

ellipticity value of each peptide at 222 nm, based on reports by Scholtz et al,[4] and values reported are based on an average of three repeats with associated standard deviations.

Chemical unfolding data were recorded by monitoring the ellipticity at 222 nm of a 30 μM peptide monomer solution in 10 mM HEPES buffer pH 7.0, in the absence and presence of 10 μM $GdCl_3$, as a function of increasing Gua-HCl concentration (from 0 to 6.0 (MB1-1L) or 6.50 (MB1-1) M) in a 1 mm path length quartz cuvette.

Thermal unfolding spectra were collected using a Jasco Peltier Temperature accessory from 25 to 85 ˚C, using a temperature gradient of 0.7 ˚C min^{-1}, monitoring the signal at 222 nm.

Luminescence Spectroscopy

Emission spectra were recorded in a 1 cm path length quartz cuvette on an Edinburgh Instruments Fluorescence FLS90 system with a 450 W Xenon arc lamp and a Hamamatsu R928 photomultiplier tube. The emission monochromator was fitted with two interchangeable gratings blazed at 500 nm and 1200 nm and the data was collected using F900 spectrometer analysis software. Aliquots of a 1 mM stock solution of $TbCl_3$ were titrated into 30 μM peptide monomer solutions in 10 mM HEPES buffer pH 7.0, and the emission profile recorded after 20 minutes equilibration. Solutions were excited at 280 nm and the emission was scanned from 455-750 nm using a 455 nm long pass filters.

Tb(III) lifetimes in D_2O and H_2O were determined for the $Tb(MB1\text{-}1L)_3$ complex, by monitoring solutions containing 10 μM $TbCl_3$ and 100 μM MB1-1 monomer in 10 mM HEPES buffer pH 7.0, using a μF flashlamp light source (50 Hz), collecting over a 10 ms range, with a lamp trigger delay of 0.1 ms. Data was fitted to mono-exponential decay kinetics in Kaleidagraph using the Marquardt-Levenburg linear least squares algorithm, and from the observed lifetime the number of coordinated water molecules was determined using the Parker-Beeby equation.[5] Data was collected in triplicate and standard deviation errors reported.

NMR Spectroscopy

Samples of 0.01, 0.02, 0.03 and 0.04 mM $GdCl_3$ in the presence of six equivalents of peptide monomer (to drive complexation) were prepared in 10 mM HEPES buffer pH 7.0.

High field relaxivity data was collected on a Bruker DMX 300 spectrometer equipped with a 7 T vertical wide-bore superconducting magnet operating at a proton resonance frequency of 300.13 MHz with a 30 mm RF bird cage coil. Data was collected and processed as previously described.[6]

Low field relaxivity data was collected on a Spinsolve Carbon benchtop NMR (Magritek, Wellington, New Zealand), equipped with a 1 T permanent magnet operating at a proton resonance frequency of 43 MHz with a 5 mm RF coil. Data was acquired using built in software with automated 90˚ and 180˚ radiofrequency pulses. T_1 data was determined using an inversion recovery pulse sequence using 2 scans with a 3.2 s acquisition time. An experiment repetition time of 15 s was used with a maximum inversion time of 10 s made up of 21 data points. T_2 data was determined using a Carr-Purcell-Meiboom-Gill pulse sequence using 4 scans with a 3.2 s acquisition time. An experiment repetition time of 7 s was used with a 2 ms echo time and a maximum total echo time of 2 s made up of 10 data points. The gradient of a plot of the relaxation rate, r_1 and r_2 (where $r_i = 1/T_i$), as a function of $Gd(MB1\text{-}1)_3$ and $Gd(MB1\text{-}1L)_3$ concentration, gives the longitudinal (r_1) and transverse (r_2) relaxivity.

^{17}O NMR Measurements

Data was acquired for 9 mM solutions of $Gd(MB1\text{-}1)_3$ in 100 mM HEPES buffer pH 7.0 (the HEPES pK_a is not pressure and temperature dependent). ^{17}O-labeled water (10%; D-Chem Ltd., Tel Aviv, Israel) was added to this solution resulting in a total enrichment of 1% ^{17}O in the studied samples. ^{17}O NMR spectra were recorded on a Bruker AVANCE DRX 400WB spectrometer equipped with a spectrospin superconducting wide-bore magnet operating at a resonance frequency of 54.24 MHz at a magnetic induction of 9.4 T. The measurements at atmospheric pressure were performed with a commercial 5 mm Bruker broadband probe thermostat with a Bruker B-VT 3000 variable temperature unit. The temperature dependence of the ^{17}O line broadening was studied over the temperature range 1.05 to 45.05 ˚C. Transverse relaxation rates were measured for the paramagnetic solutions and for the aqueous buffer solution as reference. The line widths at half height of these signals, were determined by a deconvolution procedure on the real part of the Fourier transformed spectra with a Lorentzian

shape function in the data analysis module of Bruker Topspin 1.3® software. Pressure dependent measurements were carried out with a homemade thermostat high pressure probe.[7] The sample was measured in a standard 5 mm NMR tube cut to a length of 50 mm. To enable pressure transmittance to the solution, the NMR tube was closed with a moveable macor piston. The advantage of this method is that oxygen sensitive samples can be easily placed in the NMR tube and sealed with the macor piston under an argon atmosphere. A safe subsequent transfer to the high-pressure probe is assured. The pressure was applied to the high-pressure probe via a perfluorated hydrocarbon (hexafluoropropyleneoxide, Hostinert 175, Hoechst) and measured by a VDO gauge with an accuracy of ± 1 %. Temperature was adjusted with circulating, thermostat water (Colora thermostat WK 16) to ± 0.1 ˚C of the desired value and monitored before each measurement with an internal Pt-resistance thermometer with an accuracy of ± 0.2 ˚C.

Data was fit to the following Swift-Connick equation[8]:

$$\pi \cdot 1/P_m(\Delta\nu_{obs} - \Delta\nu_{solvent}) = 1/T_{2r}$$

$$= 1/\tau_m\{(T_{2m}^{-2} + (T_{2m}\tau_m)^{-1} + \Delta\omega_m^2)/(T_{2m}^{-1} + \tau_m^{-1})^2 + \Delta\omega_m^2)\} + 1/T_{2os}$$

Activation volume ($\Delta V^{\neq}$) was obtained based on the assumption that pressure dependence of the exchange rate constant is described by the equation:

$$k_{ex} = k_{ex}^0 \exp\{(-\Delta V^{\neq}/RT) \times P\}, \text{ where P - pressure}$$

Calculation of Rotation Correlation Time for Prolate Ellipsoid Models

The rotational correlation times of MB1-1 and MB1-1L were calculated considering the peptides as prolate spheroids in Stokes Flow. The length and width of parallel three stranded coiled coils of 5 and 6 heptads, respectively, are taken from modified PDB files. Calculations were based on the standard hydrodynamic equations given by Kim and Karrila,[9] yielding rotation correlation times about the major and minor axes of 3 and 7 ns for MB1-1, and 3 and

10 ns for MB1-1L, respectively, see Table S1. More refined models of the hydrodynamic structure have since been simulated[10] and the prolate spheroid approximation is found to give an acceptably accurate prediction.

Table S1. Parameters for calculation of rotation correlation time

				dimensionless* rotational resistance coefficient about		approximate computational results for comparison:		dimensional rotation resistance coefficient about		diffusion coefficient about		rotation correlation time about	
Length (Å)	Width (Å)	major axis a	minor axis b	major axis a	minor axis b	major axis a	minor axis b	major axis a	minor axis b	major axis a (1/s)	minor axis b (1/s)	major axis a (s)	minor axis b (s)
56.3	22.3	28.15	11.15	3.03409	7.54341	3.1308	7.7069	6.8E-29	1.7E-28	6E+07	2.4E+07	2.788E-09	6.933E-09
66.6	22.3	33.3	11.15	2.10903	6.55964	2.1885	6.7113	7.8E-29	2.4E-28	5.2E+07	1.7E+07	3.209E-09	9.98E-09

Relaxivity Simulation

MATLAB R2021 software was used to simulate inner-sphere r_1 relaxivity as function of water residence time τ_m using Equations 1-3.[11]

$$r_1^{IS} = \frac{q/[H_2O]}{T_{1M} + \tau_M} \#(1)$$

$$\frac{1}{T_{1M}} = \frac{2}{15}\left(\frac{\mu_0}{4\pi}\right)^2 \frac{\hbar^2 \gamma_S^2 \gamma_H^2}{r_{MH}^6} S(S+1)\left(\frac{3\tau_c}{1 + \omega_H^2 \tau_c^2} + \frac{7\tau_c}{1 + \omega_S^2 \tau_c^2}\right) \#(2)$$

$$\frac{1}{\tau_c} = \frac{1}{\tau_m} + \frac{1}{\tau_R} \#(3)$$

where S is the spin quantum number, r_{MH} is the ion-proton distance, ω_H is the Larmor frequency of the proton, ω_S is the Larmor frequency of the electron, γ_H is the proton gyromagnetic ratio, g_e is the electronic g-factor ($g_e = 2$), μ_B is the Bohr magneton and μ_0 is the permittivity of vacuum. Static magnetic field B_0 was set to 1 T and 7 T and rotational correlation time τ_R to 2.8, 3.2, 7 or 10 ns.

2. Figure S1.

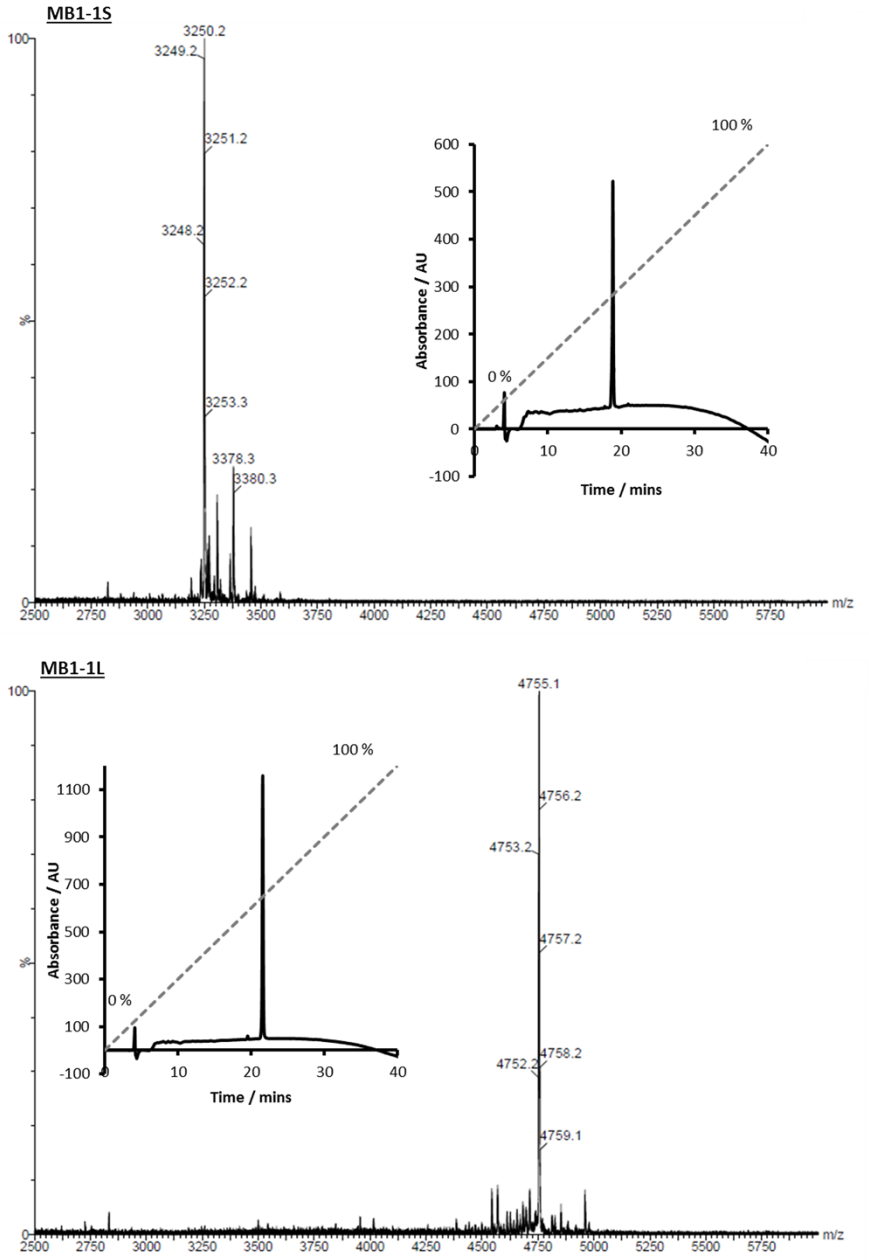

Figure S1: MALDI mass spectrum of (top) MB1-1S and (bottom) MB1-1L. Inset shows analytical reverse phase C18-HPLC chromatogram using a linear gradient from 0-100% acetonitrile in water with 0.05% TFA over 40 minutes.

3. Figure S2.

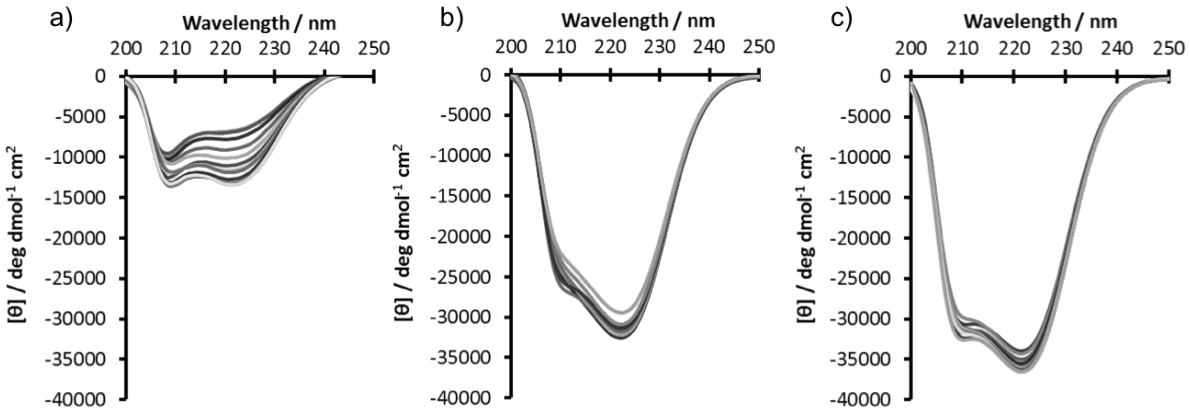

Figure S2: $GdCl_3$ titration into 100 μM a) MB1-1S, b) MB1-1 and c) MB1-1L peptide monomer in 10 mM HEPES buffer pH 7.0, monitored by CD, going from 0 μM to 100 μM $GdCl_3$ at 5 μM intervals.

4. Figure S3.

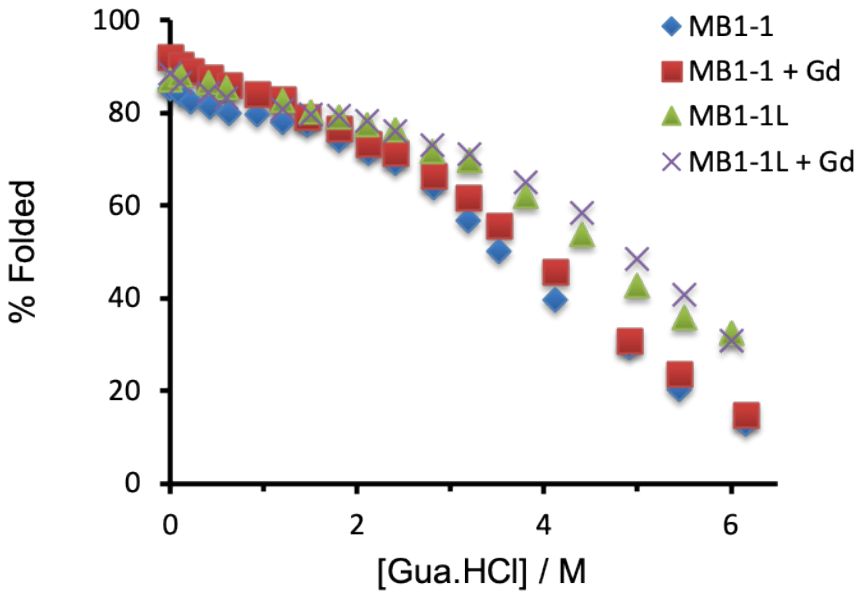

Figure S3: Percentage folded data from CD chemical unfolding of 30 μM peptide monomer +/- 10 μM $GdCl_3$ in 10 mM HEPES buffer pH 7. Concentration of Gua-HCl was increased between 0 and 6 M and the signal at 222 nm monitored. MB1-1 apo, blue diamond; MB1-1 metallo, red square; MB1-1L apo, green triangle; MB1-1L metallo, purple cross.

5. Figure S4.

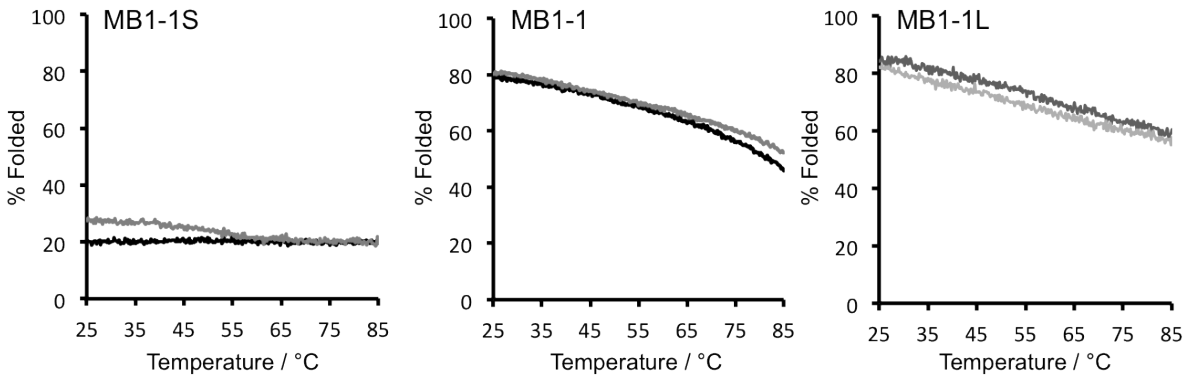

Figure S4: Percentage folded data from CD thermal unfolding of 30 μM peptide monomer in the absence (black) and presence (grey) of 10 μM $GdCl_3$ in 10 mM HEPES pH 7.0 buffer. The temperature was increased from 25 to 65˚C and the signal at 222 nm monitored.

6. Figure S5.

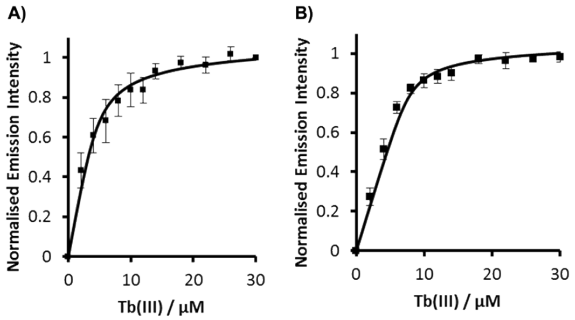

Figure S5. Plot of the normalised integration of the 545 nm Tb emission peak, for A) MB1-1 and B) MB1-1L as a function of increasing aliquots of $TbCl_3$, in 10 mM HEPES buffer pH 7.0. Fit to a peptide + $^1/_3$Gd(III) —> $^1/_3$Gd(peptide)$_3$ binding model. Error bars are standard deviation for n=3 experiments.

7. Figure S6.

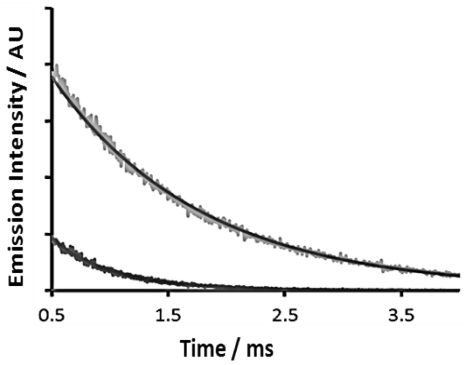

Figure S6. Representative decay profiles of Tb(III) emission at 545 nm for 100 μM MB1-1L on addition of 10 μM of Tb(III) in 10 mM HEPES buffer pH 7.0, recorded in both H_2O (light) and D_2O (dark), fit to a mono-exponential decay allowing for calculation of *q* value.

8. Figure S7.

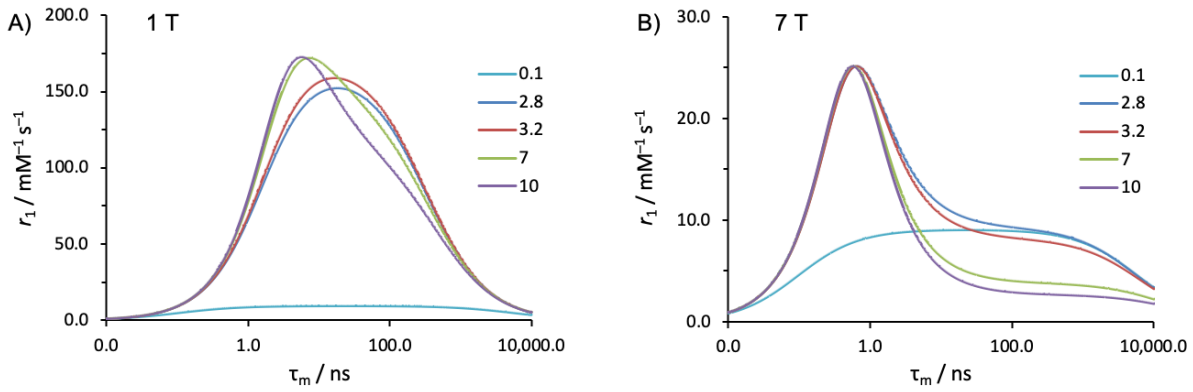

Figure S7. Predictive plots showing the effect on r_1 with changing water residency time τ_m (ns), at field strengths of A) 1 T and B) 7 T, with rotational correlation time (τ_R) of 0.1, 2.8, 3.2, 7 (MB1-1) and 10 ns (MB1-1L). Assumptions are that complexed Gd(III) is bound to three inner sphere waters, with a Gd-H distance of 3.1 Å.

9. Figure S8.

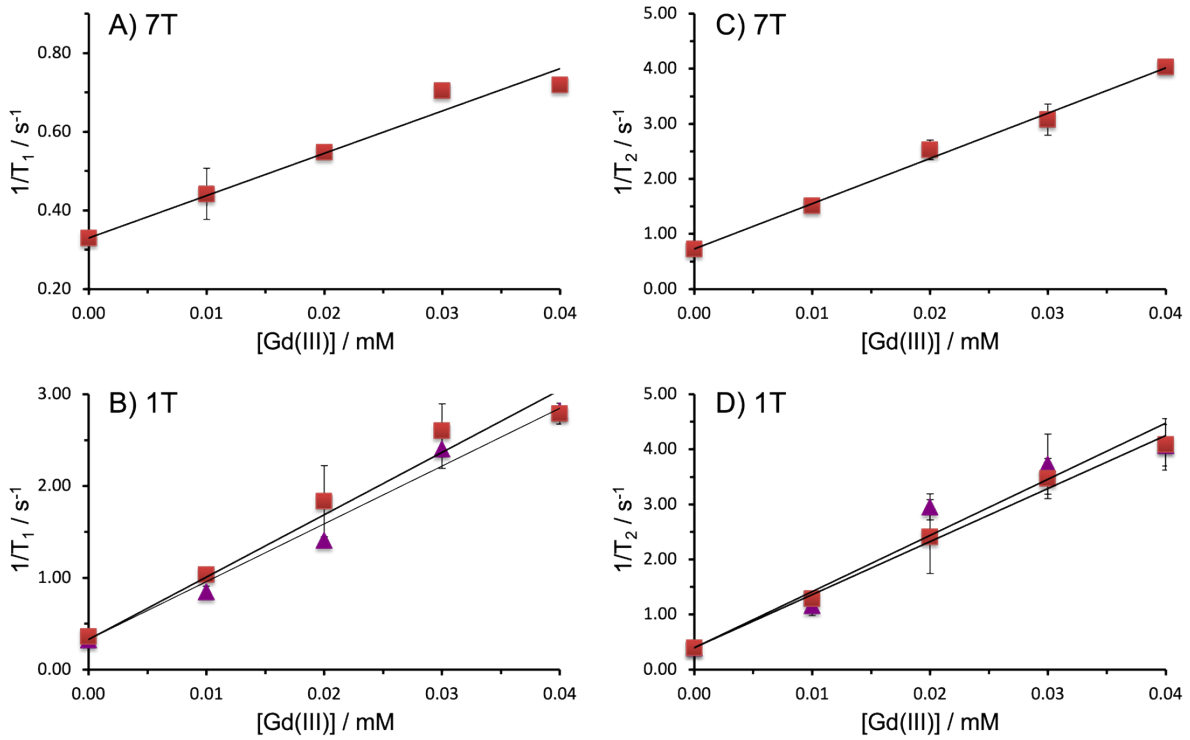

Figure S8: Relaxivity plots showing reciprocal of relaxation time as a function of Gd(III) concentration, for A/B) T_1 and C/D) T_2 relaxation rates, Gd(MB1-1)$_3$ (purple triangles in B/D) and Gd(MB1-1L)$_3$ (red squares in A/B/C/D). All samples recorded at 293 K in the presence of 10 mM HEPES buffer pH 7.0, with 2 equivalences of peptide trimer to $GdCl_3$ at A/C) 7T and B/D) 1T.

10. Figure S9.

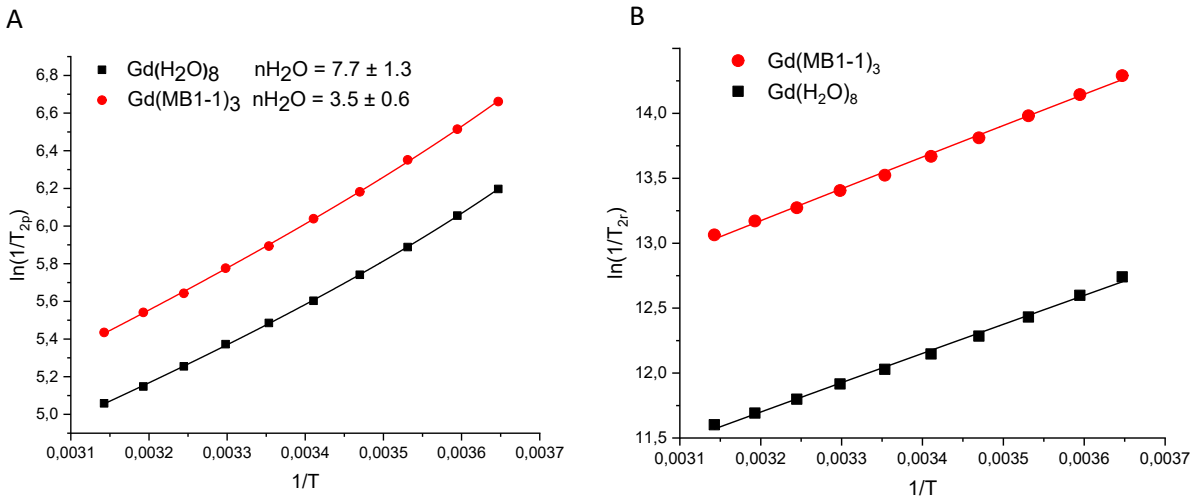

Figure S9. The temperature dependence of A) $\ln(1/T_{2p})$ and B) $\ln(1/T_{2r})$ on 1/T for 3 mM Gd(MB1-1)$_3$ in 100 mM HEPES buffer pH 7.0, B = 9.4 T in the temperature range from 274.2 to 318.2 K.

11. Figure S10.

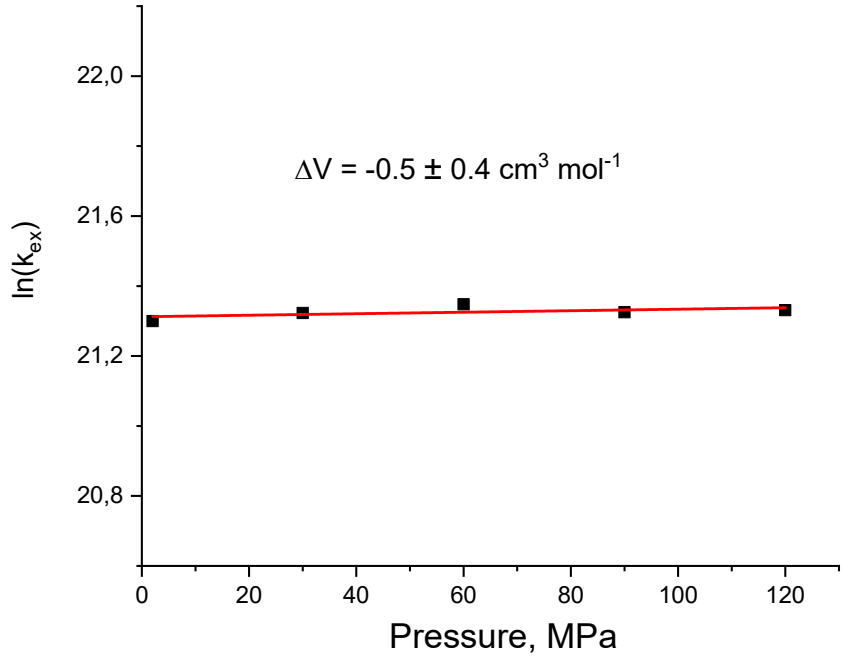

Figure S10. The pressure dependence of the ln(k_{ex}) for 3 mM Gd(MB1-1)$_3$ in 100 mM HEPES buffer pH 7.0, B = 9.4 T at 298 K.

12. Figure S11.

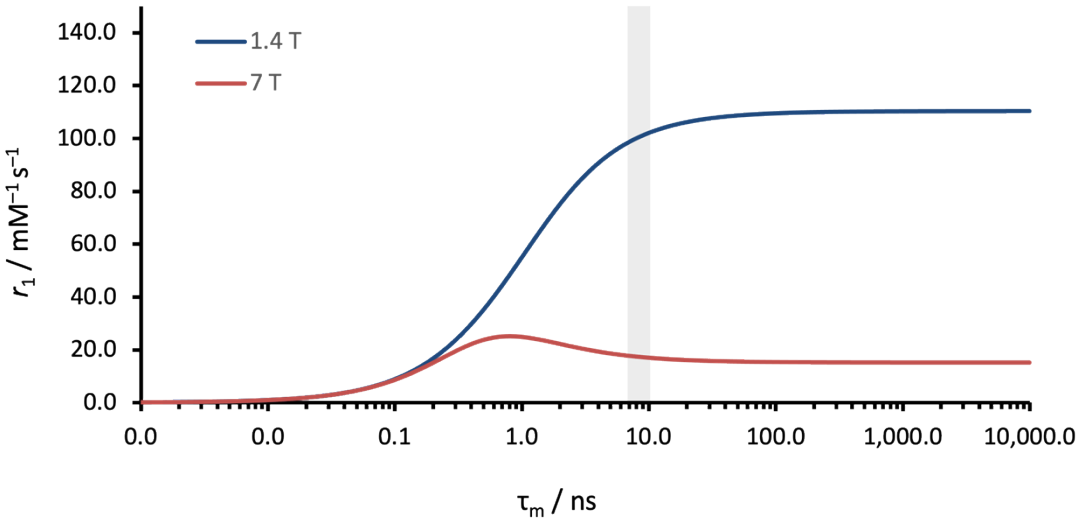

Figure S11. Predictive plots showing the effect on r_1 with changing rotational correlation time τ_R (ns), at field strengths of A) 1 T and B) 7 T, with water residency time (τ_m) of 1.56 ns. Assumptions are that complexed Gd(III) is bound to three inner sphere waters, with a Gd-H distance of 3.1 Å. Region from 7 (MB1-1) to 10 ns (MB1-1L) is highlighted in grey.

13. References

1. W. Chan and P. White, *Fmoc solid phase peptide synthesis: a practical approach*, OUP Oxford, 1999.
2. A. F. A. Peacock, G. A. Bullen, L. A. Gethings, J. P. Williams, F. H. Kriel and J. Coates, *Journal of Inorganic Biochemistry*, 2012, **117**, 298-305.
3. A. Barge, G. Cravotto, E. Gianolio and F. Fedeli, *Contrast Media Mol Imaging*, 2006, **1**, 184-188.
4. J. K. Myers, C. N. Pace and J. M. Scholtz, *Proceedings of the National Academy of Sciences*, 1997, **94**, 2833-2837.
5. A. Beeby, I. M. Clarkson, R. S. Dickins, S. Faulkner, D. Parker, L. Royle, A. S. de Sousa, J. A. Gareth Williams and M. Woods, *Journal of the Chemical Society, Perkin Transactions 2*, 1999, DOI: 10.1039/A808692C, 493-504.
6. M. R. Berwick, L. N. Slope, C. F. Smith, S. M. King, S. L. Newton, R. B. Gillis, G. G. Adams, A. J. Rowe, S. E. Harding, M. M. Britton and A. F. A. Peacock, *Chemical Science*, 2016, **7**, 2207-2216.
7. A. Zahl, A. Neubrand, S. Aygen and R. van Eldik, *Review of Scientific Instruments*, 1994, **65**, 882-886.
8. T. J. Swift and R. E. Connick, *The Journal of Chemical Physics*, 1964, **41**, 2553-2554.
9. S. Kim and S. J. Karrila, *Microhydrodynamics: principles and selected applications*, Courier Corporation, 2013.
10. D. J. Smith, *Journal of Computational Physics*, 2018, **358**, 88-102.
11. R. B. Lauffer, *Chemical Reviews*, 1987, **87**, 901-927.